ARMY RESEARCH LABORATORY

Characterization of Jets From Exploding Bridge Wire Detonators

by Daniel R. Scheffler, Matthew S. Burkins, and William P. Walters

ARL-TR-3518 May 2005

NOTICES

Disclaimers

Army Research Laboratory

Aberdeen Proving Ground, MD 21005-5066

ARL-TR-3518 **May 2005**

Characterization of Jets From Exploding Bridge Wire Detonators

Daniel R. Scheffler, Matthew S. Burkins, and William P. Walters
Weapons and Materials Research Directorate, ARL

REPORT DOCUMENTATION PAGE					Form Approved OMB No. 0704-0188

1. REPORT DATE *(DD-MM-YYYY)*	May 2005
2. REPORT TYPE	Final
3. DATES COVERED (From - To)	
4. TITLE AND SUBTITLE	Characterization of Jets From Exploding Bridge Wire Detonators
5a. CONTRACT NUMBER	
5b. GRANT NUMBER	
5c. PROGRAM ELEMENT NUMBER	
5d. PROJECT NUMBER	AH80
5e. TASK NUMBER	
5f. WORK UNIT NUMBER	
6. AUTHOR(S)	Daniel R. Scheffler, Matthew S. Burkins, and William P. Walters (all of ARL)
7. PERFORMING ORGANIZATION NAME(S) AND ADDRESS(ES)	U.S. Army Research Laboratory Weapons & Materials Research Directorate Aberdeen Proving Ground, MD 21005-5066
8. PERFORMING ORGANIZATION REPORT NUMBER	ARL-TR-3518
9. SPONSORING/MONITORING AGENCY NAME(S) AND ADDRESS(ES)	
10. SPONSOR/MONITOR'S ACRONYM(S)	
11. SPONSOR/MONITOR'S REPORT NUMBER(S)	
12. DISTRIBUTION/AVAILABILITY STATEMENT	Approved for public release; distribution is unlimited.
13. SUPPLEMENTARY NOTES	

14. ABSTRACT

A combined experimental and numerical study was conducted to characterize the jets from small exploding bridge wire detonators, which are small shaped charges. Two- and three-dimensional numerical results are compared to the experimental data.

15. SUBJECT TERMS

experiments; explosively formed penetrator; hydrocode; shaped charge jet

16. SECURITY CLASSIFICATION OF: a. REPORT	b. ABSTRACT	c. THIS PAGE	17. LIMITATION OF ABSTRACT	18. NUMBER OF PAGES	19a. NAME OF RESPONSIBLE PERSON	19b. TELEPHONE NUMBER *(Include area code)*
Unclassified	Unclassified	Unclassified	SAR	50	Daniel R. Scheffler	410-278-6017

Standard Form 298 (Rev. 8/98)
Prescribed by ANSI Std. Z39.18

Contents

List of Figures

List of Tables

Acknowledgments

The authors would like to thank Mr. Kent D. Kimsey of the U.S. Army Research Laboratory for his thorough review of this report and many helpful comments and suggestions for improving it.

INTENTIONALLY LEFT BLANK

Executive Summary

A combined experimental and numerical program was conducted at the U.S. Army Research Laboratory to characterize jets formed by three different Reynolds Industries Systems, Inc., exploding bridge wire (EBW) detonators. The detonators were designated as RP-1 SC EBW, a small (10.41-mm diameter) shaped charge (SC) with a conical liner; RP-4 SFF EBW, a 25.65-mm overall diameter detonator with a self-forging fragment (SFF) or explosively formed penetrator (EFP) liner; and RP-4 SC EBW, a 25.65-mm overall diameter detonator with a conical liner. The experimental study was conducted to determine the jet tip speeds and jet shapes. CTH[1] hydrocode simulations were also conducted to model the jet formation for each EBW detonator by means of an axis-symmetric (two-dimensional) mesh. A comparison between CTH two- and three-dimensional simulations for the RP-4 SC EBW was performed. Numerical and experimental results were compared.

[1]CTH is not an acronym.

INTENTIONALLY LEFT BLANK

1. Background

A combined numerical and experimental program was conducted at the U.S. Army Research Laboratory (ARL) to characterize small jets from conical liners and a small explosively formed penetrator (EFP) by three different off-the-shelf detonators from Reynolds Industries Systems, Inc. (RISI). The simulations were completed before the experiments. This report describes the modeling techniques used for both the conical shaped charge (SC) and EFP formation simulation. Three types of exploding bridge wire (EBW) detonators, provided by RISI, were investigated in this study. The RISI catalogue designations were RP-1 SC EBW shaped charge part number (PN) 167-8673, the RP-4 SC EBW shaped charge PN 188-7377, and the RP-4 SFF EBW self-forging fragment (SFF) PN 188-7378 (*1*). The jet properties from these charges have never been characterized. Therefore, the focus of this study sought to characterize the jets (i.e., jet shape, velocity, etc.). Figure 1 depicts the RP-1 SC EBW detonator geometry. The liner was made from copper, the sleeve from brass, and the explosive fill was pressed pentaerythrite tetranitrate (PETN). Figure 2 depicts the RP-4 SC EWB detonator geometry. The liner was a 60-degree copper cone and the explosive fill was plasticized hexogen (RDX). Figure 3 shows the geometry of the RP-4 SFF EBW detonator. The liner was made from copper and the explosive fill was plasticized RDX. Details of the liners and detonator assemblies were provided by RISI and are discussed later. The detonators were to be used in another application, which necessitated the conical SC and EFP characteristics. The other application involves using the formation simulation results to obtain the performance characteristics of the jets from the conical and EFP liners against various target scenarios.

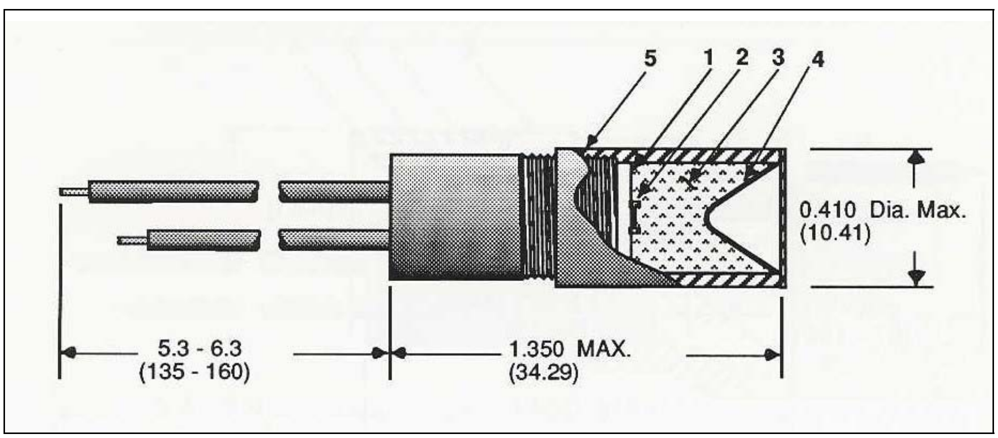

Figure 1. RP-1 SC EBW shaped charge PN 188-7355. (Parts description: 1. RP-1 standard detonator head; 2. bridgewire: gold, 0.0015 inch diameter, 0.040 inch long; 3. PETN pressed: 530 mg; 4. cone: copper; 5. sleeve: brass, 0.050 inch thick (*2*).)

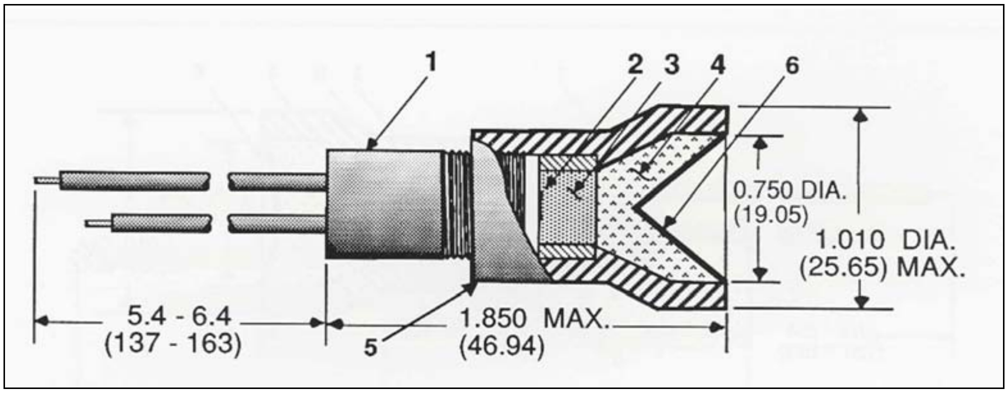

Figure 2. RP-4 SC EBW shaped charge PN 188-7377. (Parts description: 1. RP-1 standard detonator head; 2. bridgewire: gold, 0.0015 inch diameter, 0.040 inch long; 3. initiating explosive: 92 mg of PETN; 4. high density explosive: 3.44 g of plasticized RDX; 5. sleeve, 6. liner: copper, 60 degrees by 0.020 inch thick (*2*).)

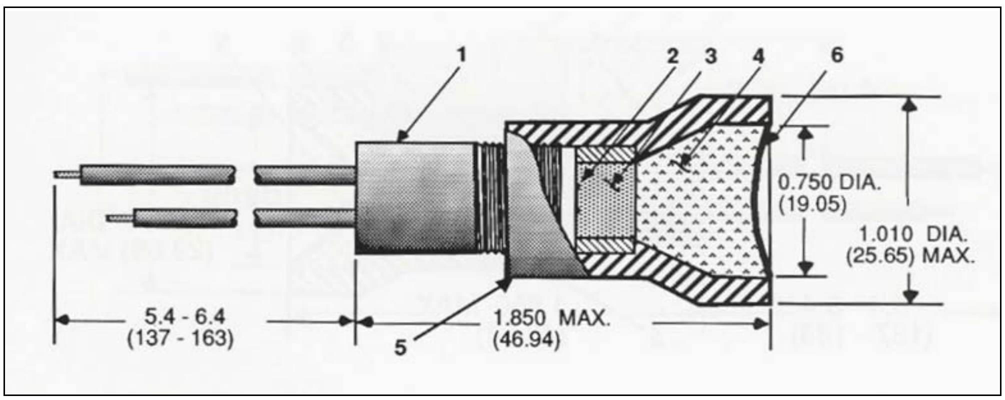

Figure 3. RP-4 SFF EBW self-forging fragment PN 188-7378. (Parts description: 1. RP-1 standard detonator head; 2. bridgewire: gold, 0.0015 inch diameter, 0.040 inch long; 3. initiating explosive: 92 mg of PETN; 4. high density explosive: 6.03 g of plasticized RDX; 5. sleeve, 6. liner: copper, 0.020 inch thick (*2*).)

2. Experiments

The testing was performed at ARL's experimental facility 108 at Aberdeen Proving Ground, Maryland, since this was the only facility available for this program. Three 150-kilo-electron volt (keV) x-ray tubes were placed 4 inches (102 mm) apart along a horizontal axis. The charge was positioned so that it pointed perpendicular to the x-ray axis at the location of the middle x-ray head. Because of limitations of the experimental facility, only 10 inches (254 mm) of vertical film coverage was possible. For the RP1 SC EBW detonator, in particular, the radiographic measurements were extremely difficult to resolve because of the extremely small particle size produced by the charge.

The jet and EFP free flight flash radiographs are shown in figures 4 through 9. Figures 4 through 6 show the flash radiographs for the RP-1 SC EBW for shot numbers 814, 815, and 817, respectively. The radiographs show that the RP-1 SC EBW is not a well-formed shaped charge jet (SCJ) in that the jet particles were not collinear. In addition, the experimentally determined jet tip velocities vary significantly, as listed in table 1. The jet tip velocity was determined to range from 2,653 to 4,867 m/s plus or minus the error measurement. This is because of limitations of the experimental facility, the fact that the shaped charges were not precision manufactured, and difficulty in the determination of the exact location of the leading particle in the radiographs.

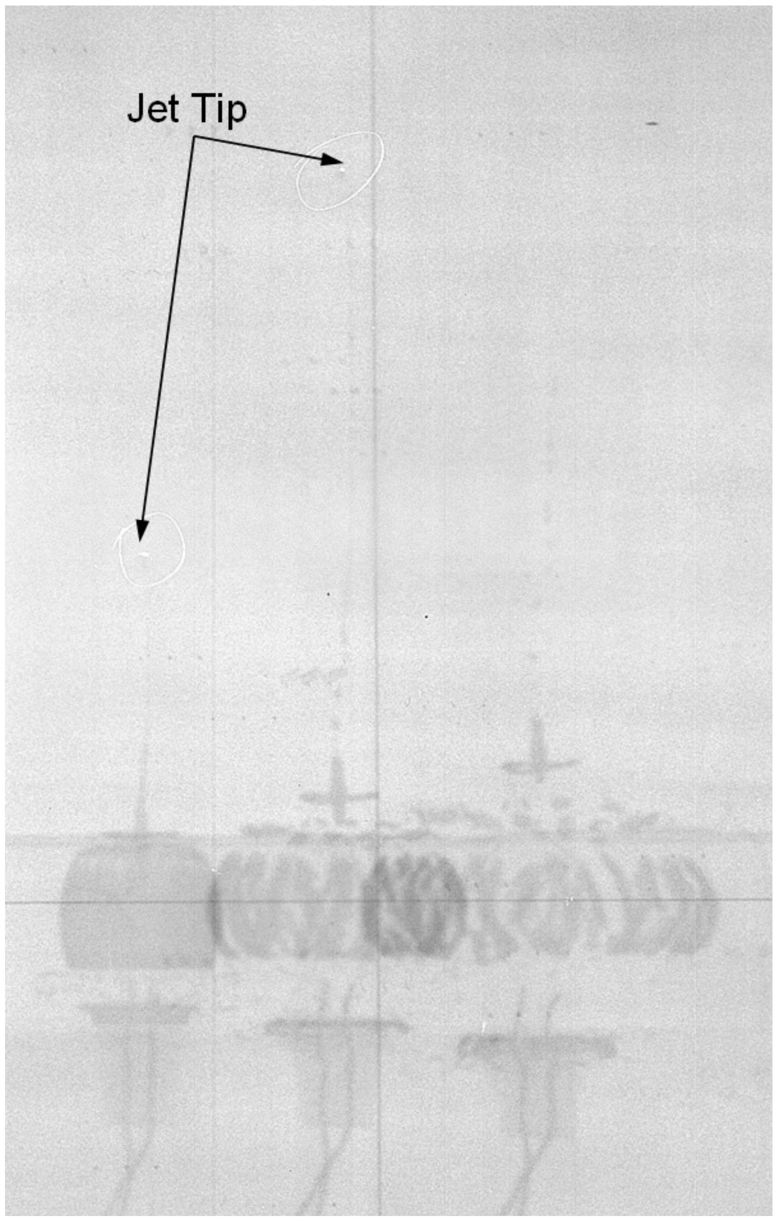

Figure 4. RP-1 SC EBW shot No. 814. (X-ray flash times are 13.7, 23.6, and 33.6 μs.)

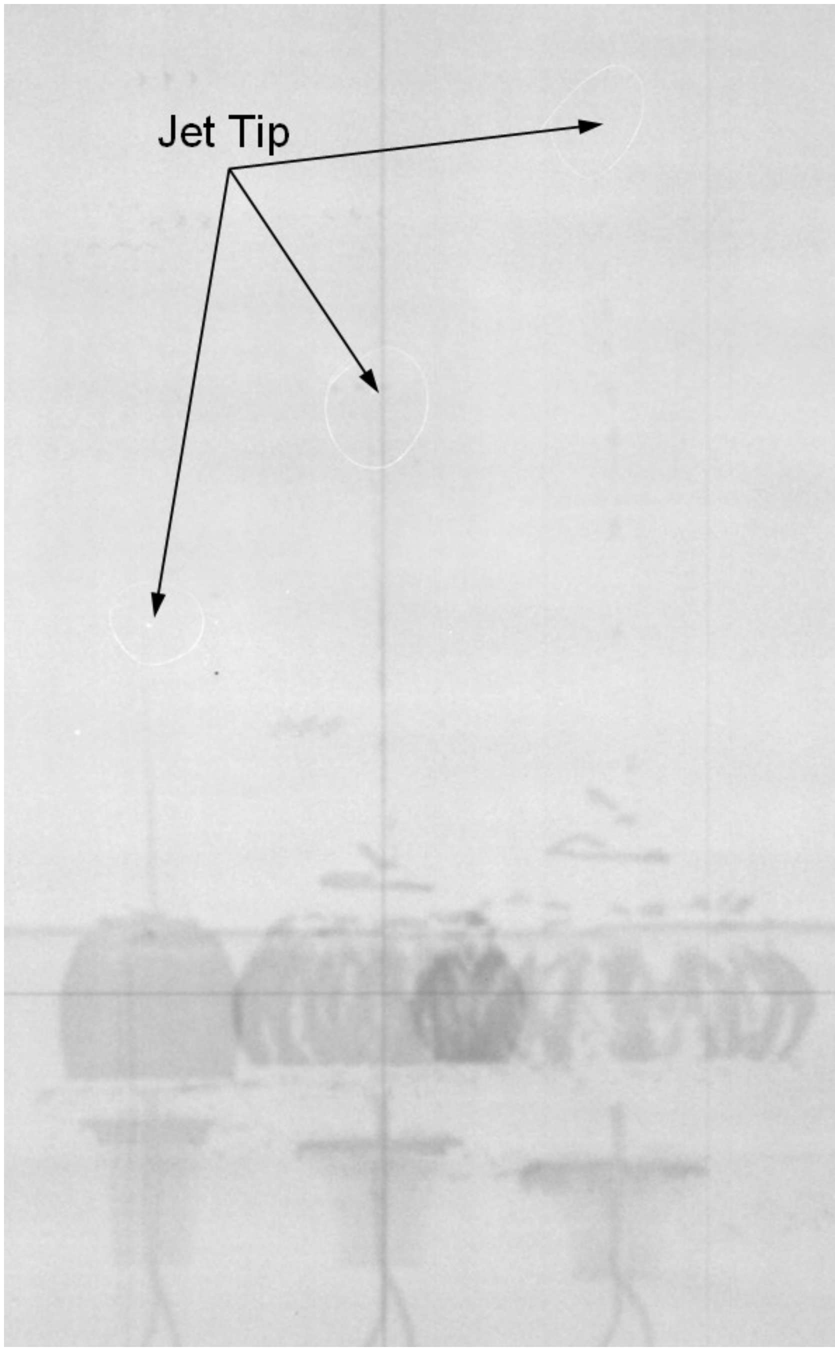

Figure 5. RP-1 SC EBW shot No. 815. (X-ray flash times are 13.6, 23.5, and 33.5 µs.)

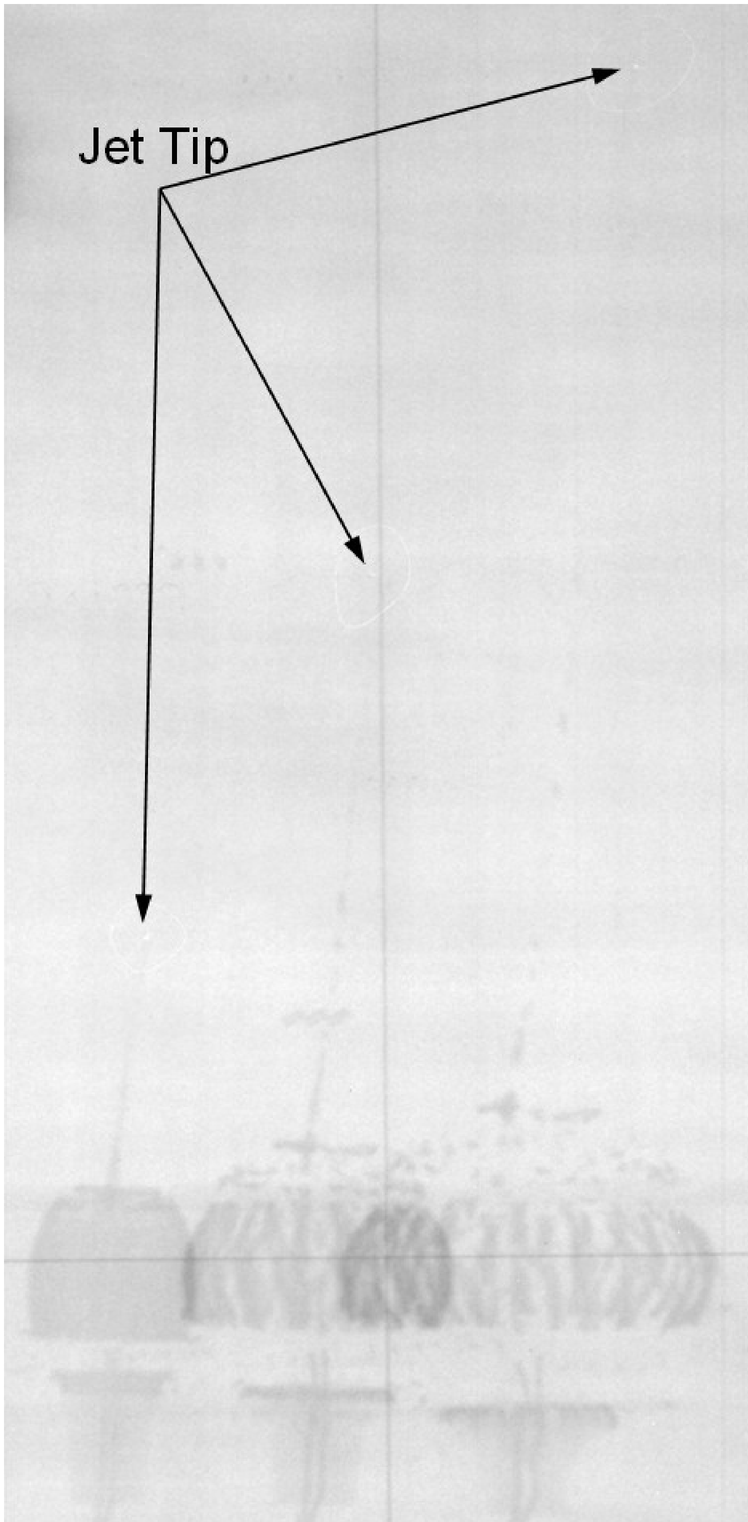

Figure 6. RP-1 SC EBW shot No. 817. (X-ray flash times are 13.4, 23.4, and 33.5 µs.)

Figure 7 shows the free flight jet for the RP-4 SC EBW at three radiograph flash times. The figure shows that the RP-4 SC EBW produces a well-formed jet. The jet remains relatively collinear and cohesive. At 23.6 µs, some necking near the rear of the jet is evident. The jet tip velocity was determined to be around 5,313 m/s (see table 1). The jet diameter for this charge was requested by RISI, and the measured jet diameter was 3.1 mm at the tip, 1.05 mm in the middle of the jet, and 3.0 mm at the tail. These values were measured at the latest flash time (23.6 µs), but the jet was still stretching.

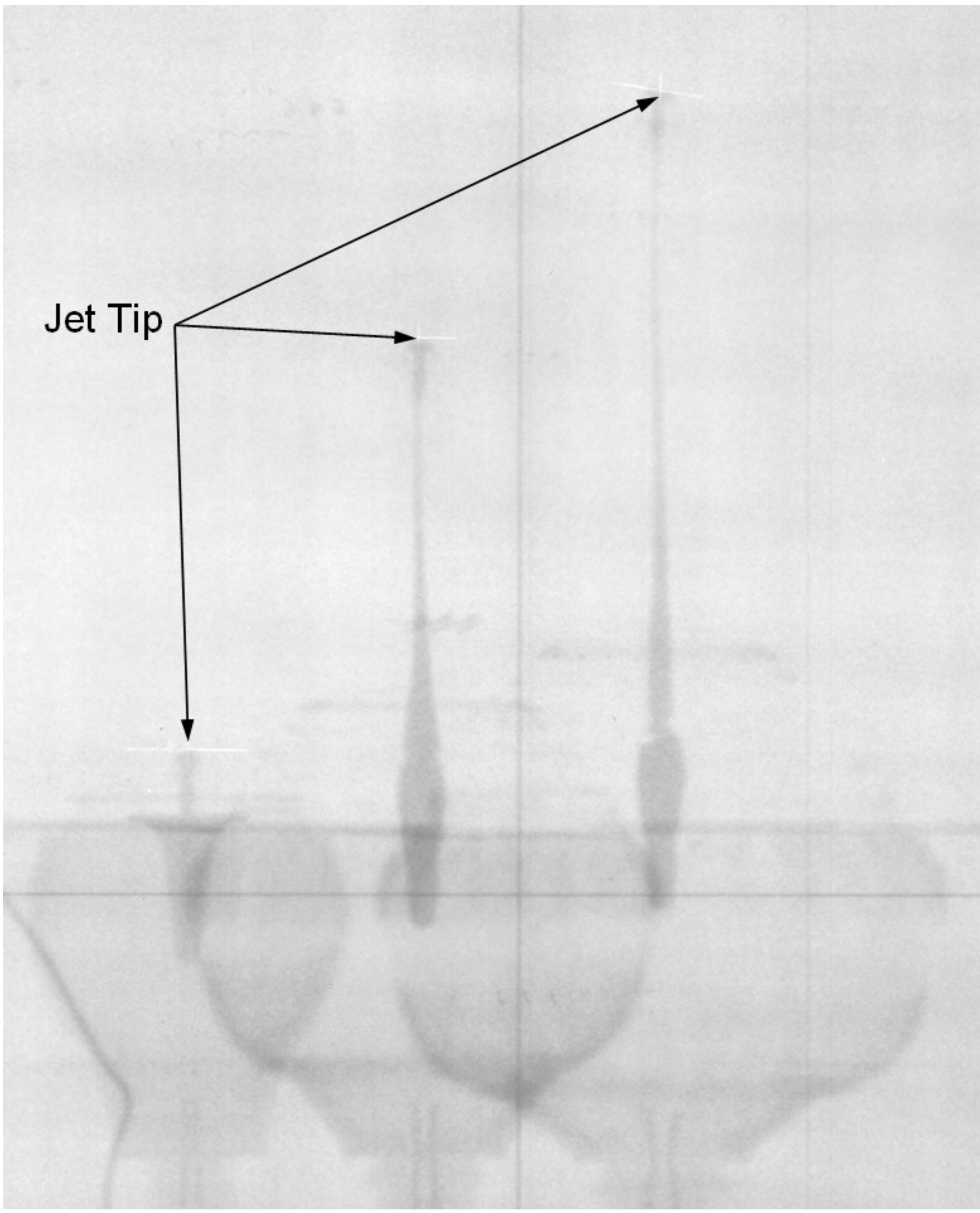

Figure 7. RP-4 SC EBW shot No. 816. (X-ray flash times are 10.7, 18.7, and 23.6 µs.)

Figures 8 and 9 show the free flight EFP for the RP-4 SFF EBW charge with the radiograph flash times given in the figure captions, for shot numbers 779 and 778, respectively. Figure 8 shows the EFP in the early stages of formation and figure 9 shows the EFP at the later stages of formation. The velocity of the leading edge of both is between 2,900 and 3,000 m/s (see table 1). Figures 8 and 9 show that although the leading edge velocity of the EFP is fairly consistent, the EFP's final shape can vary considerably.

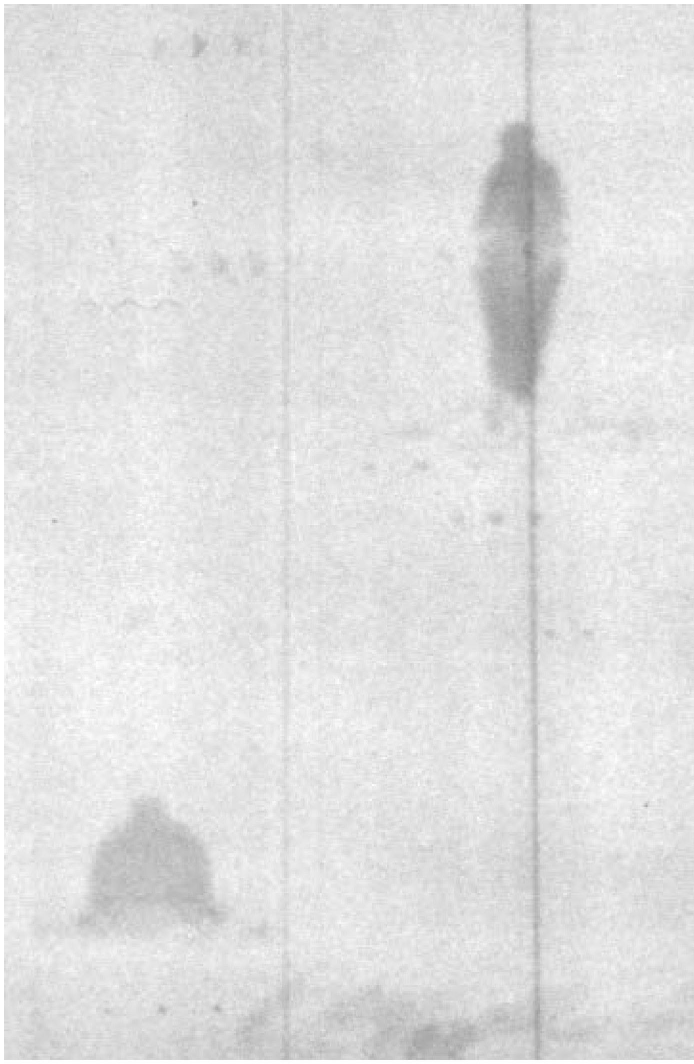

Figure 8. RP-4 SFF EBW shot No. 779. (X-ray flash times are 15.1 and 30.7 µs.)

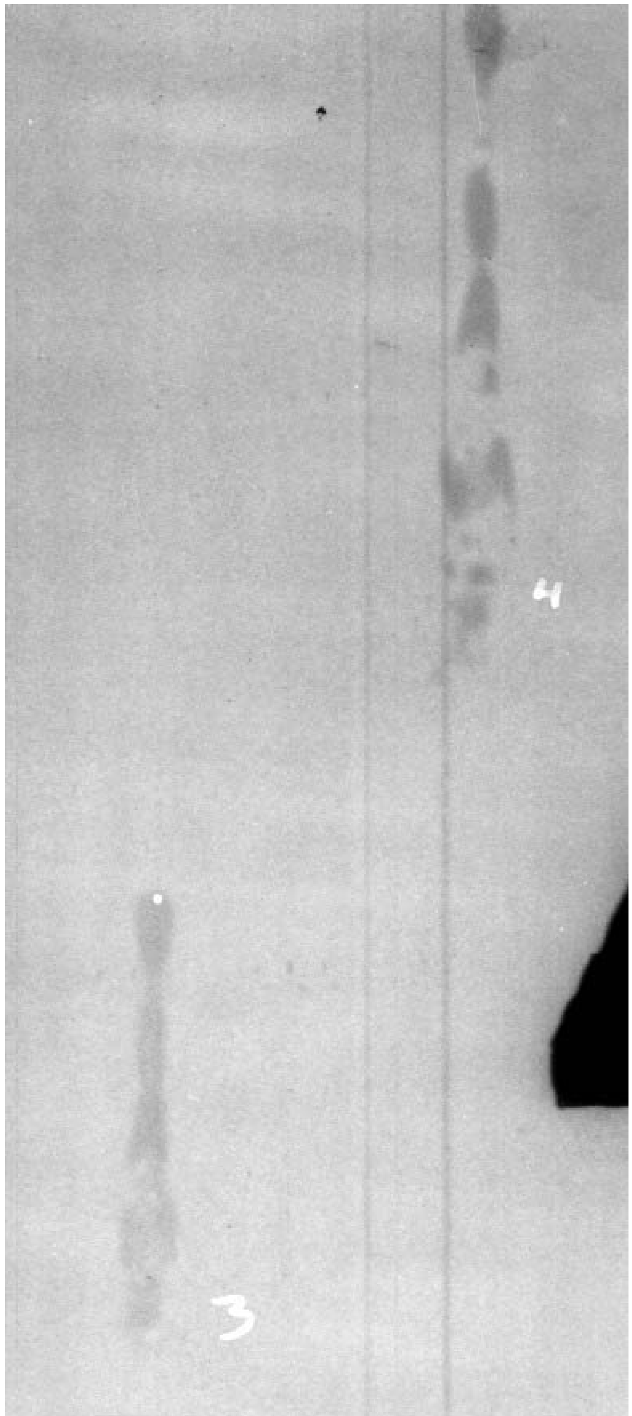

Figure 9. RP-4 SFF EBW shot No. 778. (X-ray flash times are 50.6 and 75.5 µs.)

Table 1. Experimental results.

RP-1 SC EBW		
Shot No.	**Jet Tip Velocity (m/s)**	**Error (m/s)**
814	4867	±147
815	2653	±53
817	4243	±133
RP-4 SC EBW		
Shot No.	**Jet Tip Velocity (m/s)**	**Error (m/s)**
816	5313	±125
RP-4 SFF EBW		
Shot No.	**Tip Velocity (m/s)**	**Error (m/s)**
778	2984	±36
779	2953	±51

Any significant errors in the charge velocities can be attributed to three main sources of error: 1) placement of the charge with reference to the x-ray tubes, 2) measurements from the radiographs, and 3) the measurement of time between the x-ray flashes. The placement errors included translational errors in the X and Y planes, as well as rotational errors attributable to angular departure from perfectly plumb. These placement errors totaled approximately 1/8 inch (3.2 mm) and contributed to changes in the correction factor used to remove the magnification of the radiographic images. The error for the film measurements was ±0.010 inch (0.25 mm) per measurement. The timing error was 1×10^{-7} seconds for each measurement. In general, we obtained the velocities by dividing a small distance by a short time, thereby magnifying the effect of the accumulated errors. Based on the errors just discussed, the jet tip or EFP velocities and associated errors are given in table 1.

3. Simulation Setup

Three two-dimensional (2-D) axis-symmetric simulations were conducted with a fine resolution mesh, one for each detonator type. An additional three-dimensional (3-D) simulation of the jet formation was performed for the RP-4 SC EBW SC with the same cell size of the coarse resolution mesh needed for 3-D simulations involving a target. Thus, the 3-D simulation would be used to determine whether the coarse mesh would still adequately model small jets.

The simulations were performed with the March 1999 version of the CTH hydrocode (*2*), which is a state-of-the-art, second order accurate, Eulerian hydrocode undergoing continuous development at the Sandia National Laboratories, Albuquerque, New Mexico. CTH is capable of solving complex problems in shock physics in one, two, or three dimensions. The code provides several constitutive models, including an elastic-perfectly plastic model with provisions for work hardening and thermal softening, the Johnson-Cook model (*3*), the Zerrilli-Armstrong model (*4*), the Steinberg-Guinan-Lund model (*5*, *6*), an undocumented power-law model, and others. High explosive detonation can be modeled via the programmed burn model, the Chapman-Jouguet volume burn models, or the history variable reactive burn model (*7*). Several equation-of-state (EOS) options are available, including tabular (i.e., SESAME[2]), analytical equation of state (ANEOS), Mie-Grüneisen, and Jones-Wilkins-Lee (JWL) (*8*). Material failure occurs when a threshold value of tensile stress or hydrostatic pressure is exceeded. In addition, the Johnson-Cook fracture model (*9*) is available. When failure occurs in a cell, void is introduced until the stress state of the cell is reduced to zero. Recompression is permitted. To reduce the diffusion typically encountered in Eulerian simulations, several advanced material interface tracking algorithms are provided, including the high-resolution interface tracking algorithm (available for 2-D simulations only), the simple line interface calculation algorithm (*10*), and the Sandia-modified Young's reconstruction algorithm (*11*).

Initial simulations of the SCJs and EFP were performed in 2-D axis-symmetric configuration. The RP-4 SC EBW was repeated with quarter symmetry in a 3-D model with a mesh resolution similar to that needed to model jet-target impacts. The detonator geometries used in the CTH simulations for the RP1 SC EBW, RP4 SC EBW, and RP4 SFF EBW were simplified from the drawings shown in figures 10 through 12. The origin of the coordinate system used in all simulations was placed at the base of the liner. For the axis-symmetric simulations, the mesh consisted of 650×6600 cells for the RP1 SC EBW simulation and 1500×7500 cells for both the RP4 SC EBW and RP4 SFF EBW simulations. The cell size for all axis-symmetric simulations was 0.001×0.001 cm and was uniform throughout the meshes. The 3-D RP4 SC EBW mesh consisted of $150 \times 750 \times 150$ cells having a uniform size of $0.01 \times 0.01 \times 0.01$ cm with planes of symmetry at x = 0 and z = 0. A Lagrangian tracer particle was placed at the origin of the coordinate system of each simulation to capture the jet tip or EFP leading edge velocity.

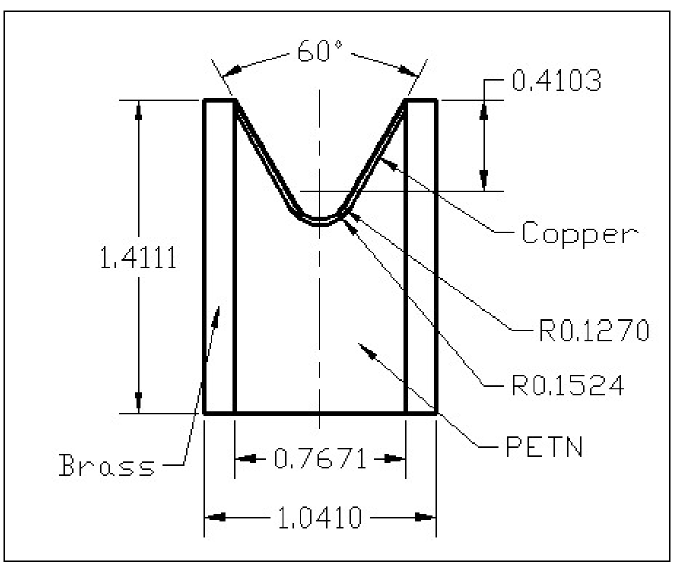

Figure 10. RP-1 SC EBW geometry used for simulation.
(Dimensions are in centimeters.)

[2]Not an acronym

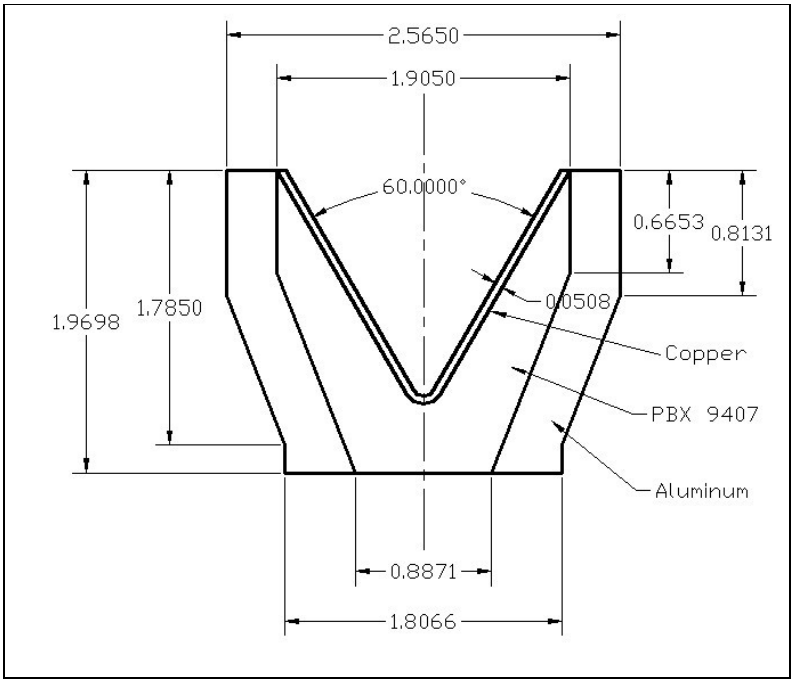

Figure 11. RP-4 SC EBW geometry used for simulation. (Dimensions are in centimeters.)

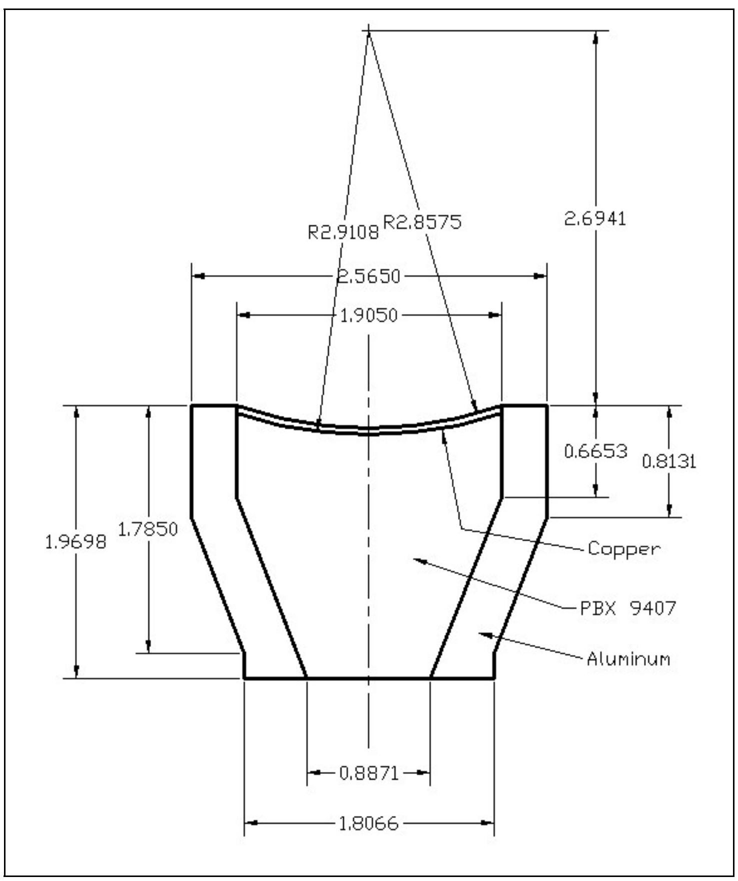

Figure 12. RP-4 SFF EBW EFP geometry used for simulation. (Dimensions are in centimeters.)

The copper liners were modeled with standard copper properties for the Johnson-Cook constitutive model and CTH library values for the Mie-Grüneisen EOS. The same holds true for the brass case for the RP1 SC EBW simulation. The aluminum case for the RP4 SC EBW and RP4 SFF EBW simulations was modeled with the Johnson-Cook constitutive model and the SESAME tabular EOS available in the CTH material library. Failure in the metals was modeled with a simple tensile pressure criterion so that failure for copper, brass, and aluminum would occur when the tensile pressure would exceed 0.345, 1.300, and 0.400 GPa, respectively. The explosives, PETN and plastic-bonded explosive (PBX) 9407, were treated as fluids (i.e., they do not support strength). The JWL EOS was used to model the pressure-volume-energy behavior of the detonation products with parameters reported by Dobratz (12). A simple programmed burn model was used to model explosive initiation. In the axis-symmetric simulations, the explosive was initiated along a line at the bottom of the explosive and in the 3-D simulation, the explosive was initiated at a disk at the bottom of the explosive. A complete listing of the CTH input for the axis-symmetric simulations for the RP1 SC EBW, RP4 SC EBW, and RP4 SFF EBW is given in appendices A through C, respectively. The CTH input for the 3-D simulation of the RP4 SC EBW is shown in appendix D.

4. Results and Discussion

4.1 RP-1 SC EBW Simulation

Figure 13 shows the jet formation of the RP-1 SC EBW charge at times that roughly correspond to the times shown in the flash radiographs in figures 4 through 6. Like the jet in the experiments, the jet particulates early. Figure 14 shows the axial velocity profile of the jet at 13 µs. The jet tip velocity is 3.3 km/s, which is within the range of tip velocities listed in table 1. The RP-1 SC EBW charge produced a poorly formed jet.

4.2 RP-4 SC EBW Simulations

Figure 15 shows the RP-4 SC EBW 2-D axis-symmetric simulation results at 0, 11, and 19 µs. These free flight times were chosen to roughly match the flash radiographs in figure 7. The general shape of the jet in both the experiment and the simulation agrees. However, there seems to be a time mismatching between the experiment and simulation. Time zero for the simulation corresponds to when the explosive was line initiated at the base of the explosive charge, as shown in figure 11. Time zero in the experiments corresponds to when an electrical current was applied to the standard detonator head (item 1 in figure 2). Thus, the time-zero offset suggests that the simulation times correspond to later experimental times. It is estimated that the difference between the experiments and simulation is about 5 µs.

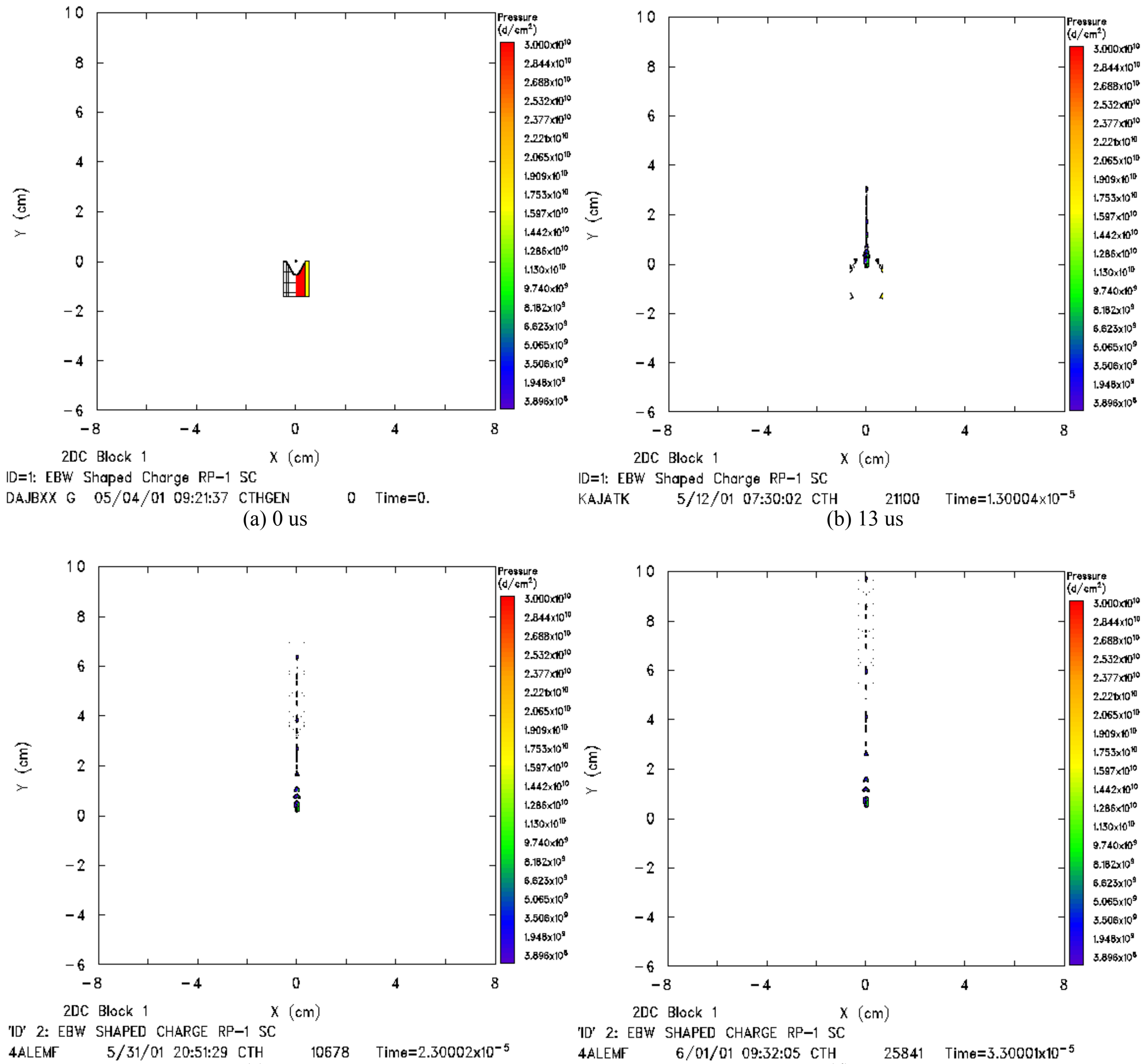

(a) 0 us (b) 13 us (c) 23 us (d) 33 us

Figure 13. RP-1 SC EBW jet formation at (a) 0 µs , (b) 13 µs, (c) 23 µs, and (d) 33 µs.

Figure 16 shows the RP-4 SC EBW 3-D simulation results at 0 and 11 µs. The purpose of this simulation was to determine whether a coarser 3-D mesh could accurately capture the jet formation and jet tip velocity, since a coarse mesh would be needed to model jet-target interactions. A comparison of figures 15(b) and 16(b) indicates little difference between the jet formation of the 2-D and 3-D simulations. Thus, the mesh for the 3-D simulation is adequate. Figure 17 shows the axial jet velocity profile of the RP-4 SC EBW charge at 12 µs for the 2-D and the 3-D simulations. Note that there are only minor differences in the velocity profile, most notably at the leading edge of the jet. The jet tip velocity was determined to be 5.7 km/s for the

2-D simulation, while it was 5.6 km/s for the 3-D simulation. Thus, the simulations over-predict the experimentally determined tip velocity, 5.313 ±0.125 km/s, by approximately 7%. However, with only one experiment, the data scatter is unknown.

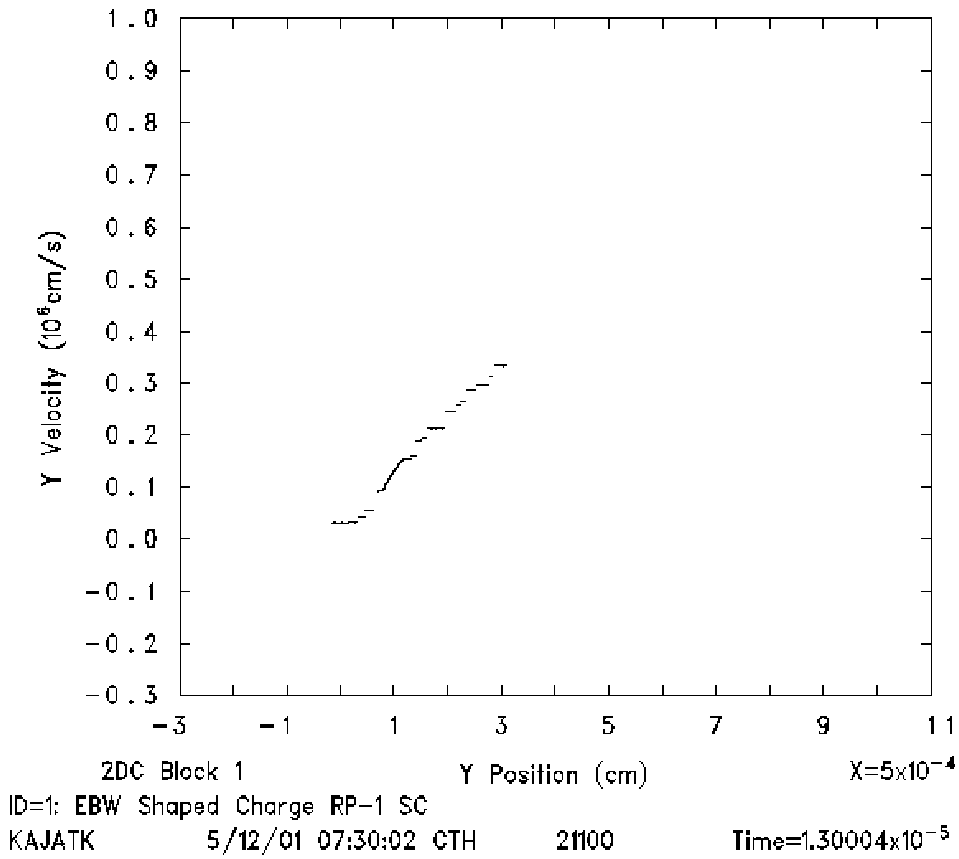

Figure 14. RP-1 SC EBW axial jet velocity profile at 13 µs.

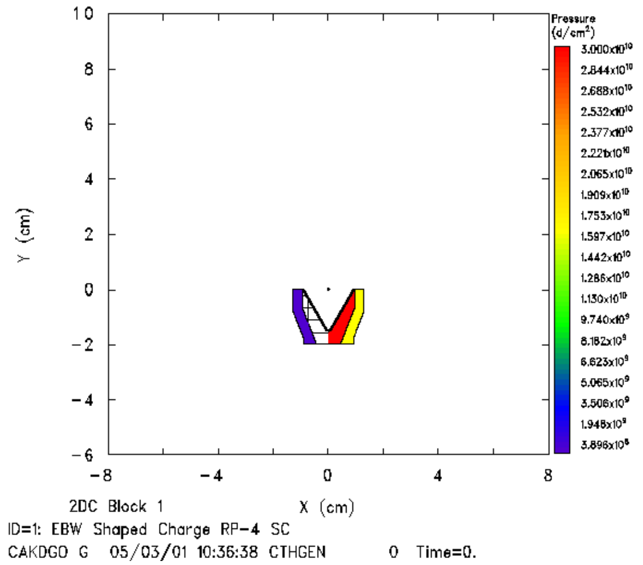

(a) 0 us

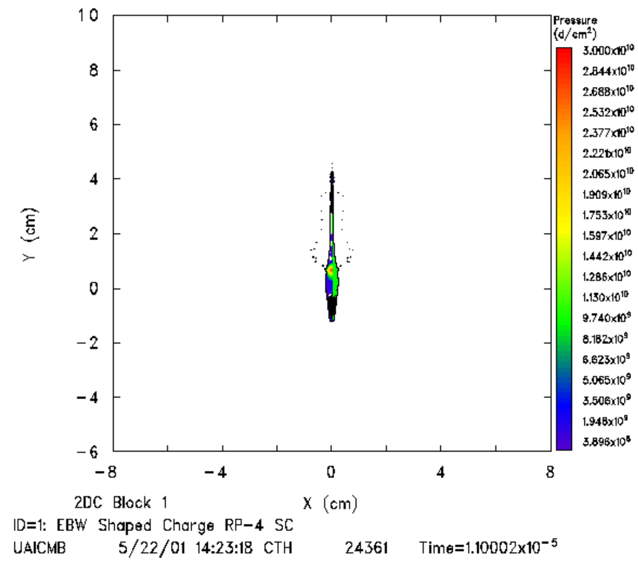

(b) 11 us

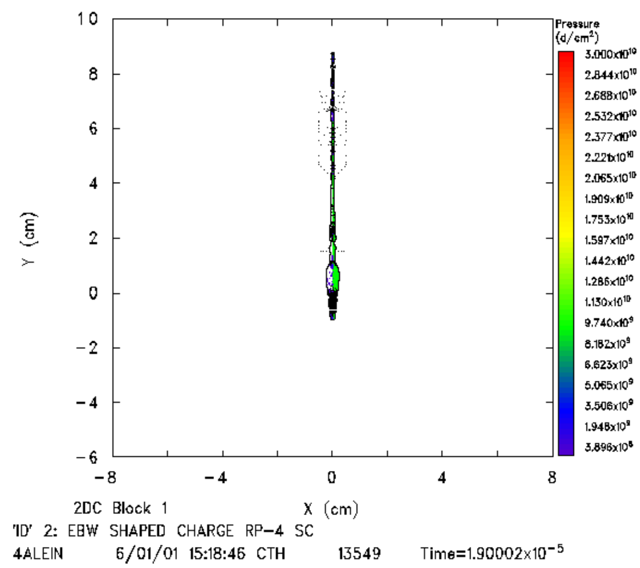

(c) 19 us

Figure 15. RP-4 SC EBW jet formation at (a) 0 μs , (b) 11 μs, and (c) 19 μs.

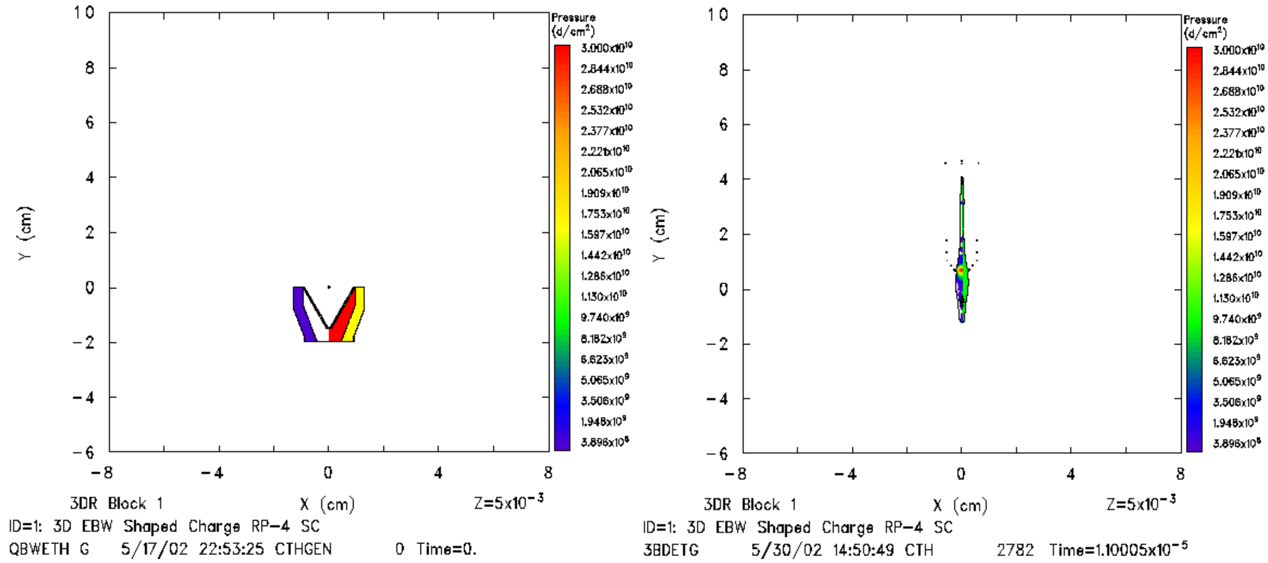

(a) 0 us **(b) 11 us**

Figure 16. RP-4 SC EBW 3-D jet formation at (a) 0 µs and (b) 11 µs.

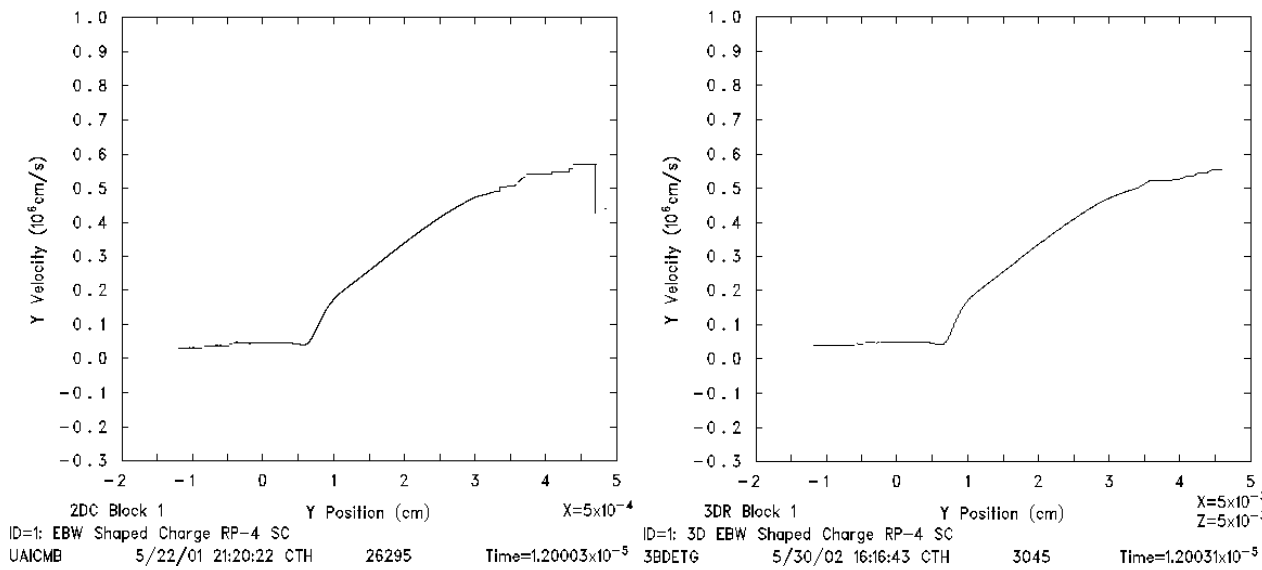

(a) 2-D **(b) 3-D**

Figure 17. RP-4 SC EBW jet velocity profile shown 12 µs for (a) 2-D and (b) 3-D simulation.

4.3 RP-4 SFF EBW Simulation

Formation of the EFP is shown in figure 18 at times that roughly correspond to the experimental radiograph flash times in figures 8 and 9. Again, there is some difference in time because of the difference in time zero between the experiments and the simulation, with the simulation time being later than the experiments. The estimated time difference is about 5 µs. At 20 µs, a global velocity transformation was performed to subtract 2.9 km/s in the axial direction from the mesh to freeze the EFP's forward motion while allowing it to continue to deform, thereby minimizing the size of the mesh needed to complete the simulation to 50 µs. The leading edge velocity determined from the simulation was 2.8 km/s and agrees very well with the velocities determined from two experiments (see table 1). The EFP shape shown in figures 8 and 9 varies a great deal. These experiments show that the RP-4 SFF EBW detonator forms penetrators that fail to create a consistent shape. Thus, it is difficult to say how well the EFP shape determined from simulation agrees with the experiments.

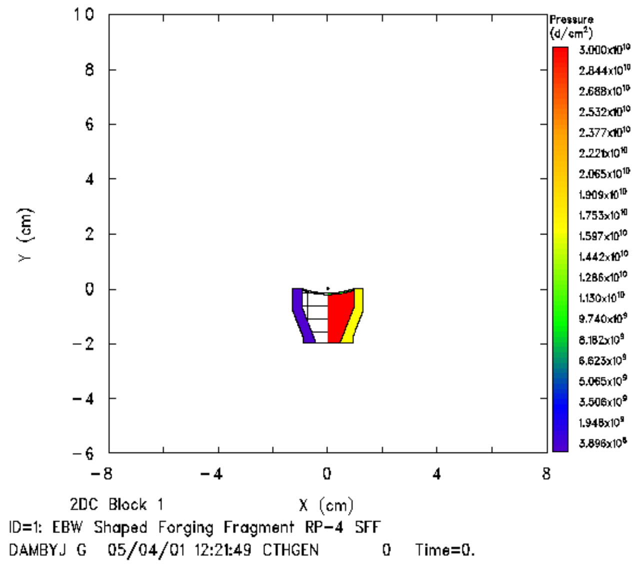

(a) 0 us

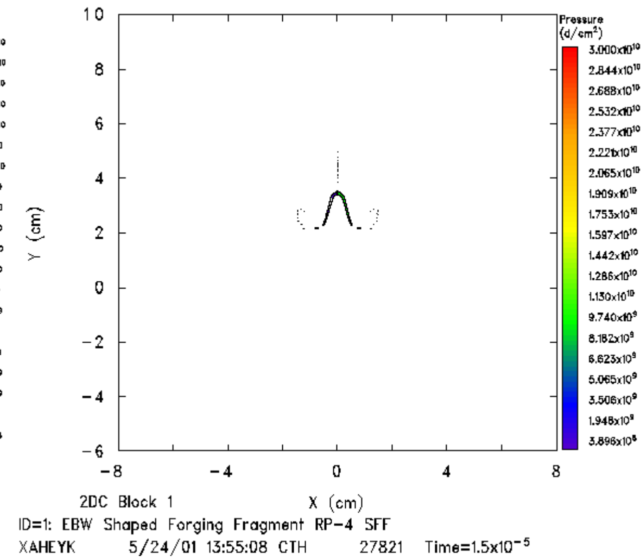

(b) 15 us

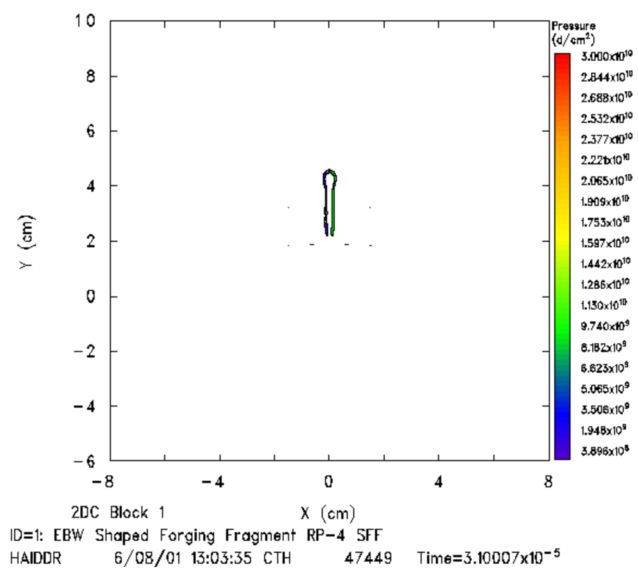

(c) 0 us

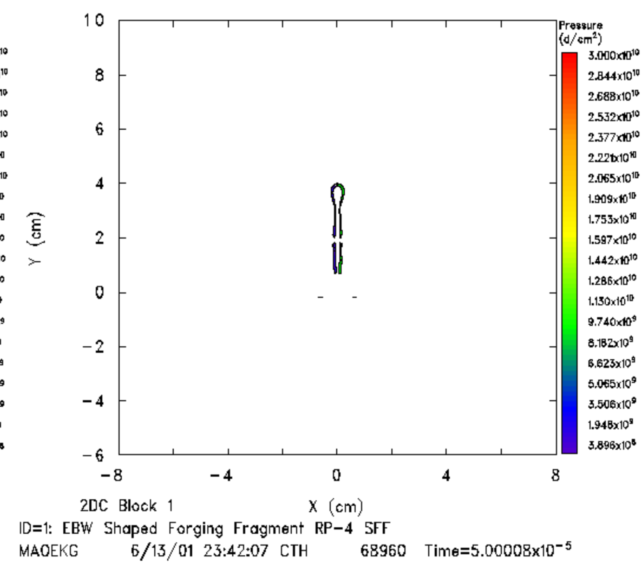

(d) 15 us

Figure 18. RP-4 SFF EBW EFP formation at (a) 0 µs , (b) 15 µs, (c) 31 µs, and (d) 50 µs.

5. Conclusions

The results of numerical simulations of the free flight characteristics of two conical SC and one EFP were presented. The charges were on the order of 1 inch in diameter. The simulations were compared to experimental data and were performed in advance of the experiments. The 2-D jet formations were simulated with a very fine Eulerian computational mesh. A 3-D simulation involving a target impact scenario would require a much coarser computational mesh. The results for both the 2-D and 3-D simulations of the RP-4 SC EBW are in good agreement.

The off-the-shelf detonators were not precision manufactured devices, and thus, there was a lot of scatter in the experimental data. The RP-1 SC EBW jet particles do not remain collinear nor do they have a consistent jet tip velocity. The jet tip velocity obtained numerically fell within the scatter of the experimental data. The RP-4 SC EBW detonator produced a well-formed jet, as observed in the experiment and simulations. Based on one experiment for the RP-4 SC EBW detonator, free flight jet characteristics such as overall shape and tip velocity show good agreement between the experiment and simulations. The tip velocity of the EFP (RP-4 SFF EBW detonator) predicted by the simulation is also in good agreement with the limited experimental results.

Generally, the CTH simulations predicted jet characteristics that are in good agreement with the limited experimental data for off-the-shelf EBW detonators.

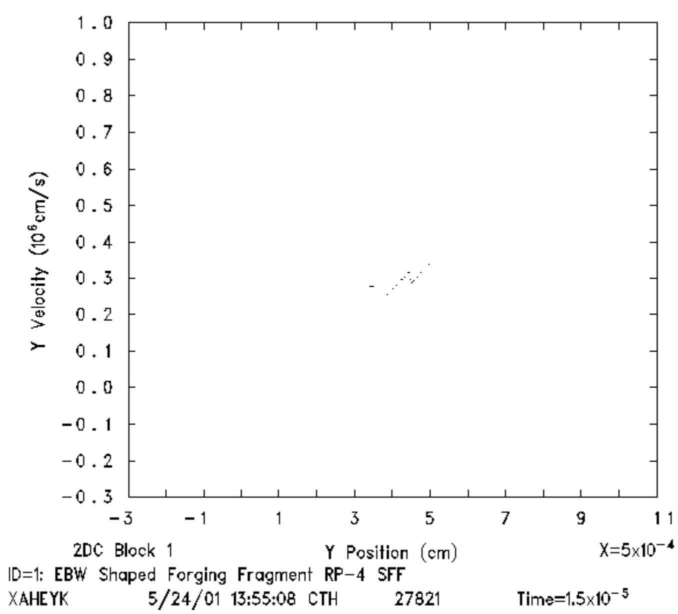

Figure 19. RP-4 SFF EBW axial EFP velocity profile at 15 μs.

6. References

1. Reynolds Industries Systems, Incorporated. Secondary Explosive Initiators & Accessories. Catalogue.

2. Mc Glaun, J. M; Thompson, S. L.; Elrick, M. G. CTH: A Three-Dimensional Shock Wave Physics Code. *International Journal of Impact Engineering* **1990**, *1–4*, 351–360.

3. Johnson, G. R.; Cook, W. H. A Constitutive Model and Data for Metals Subjected to Large Strains, High Strain Rates, and High Temperatures. *Proceedings of the Seventh International Symposium on Ballistics*, The Hague: The Netherlands, 1983.

4. Zerilli, F. J.; Amstrong, R. W. Dislocation-Mechanics-Based Constitutive Relations for Material Dynamics Calculations. *Journal of Applied Physics* **1987**, *5*, 1816–1825.

5. Steinberg, D. J.; Lund, C. M. A Constitutive Model for Strain Rates From 10^{-4} to 10^{6} s^{-1}. *Journal of Applied Physics* **1989**, *4*, 1528–1533.

6. Steinberg, D. J.; Cochran, S. G.; Guinan, M. W. A Constitutive Model for Metals Applicable at High-Strain Rate. *Journal of Applied Physics* **1980**, *3*, 1498–1504.

7. Kerley, G. I. *CTH Equation of State Package: Porosity and Reactive Burn Models*; SAND92-0553; Sandia National Laboratories: Albuquerque, NM, 1992.

8. Lee, E. L; Hornig, H. C.; Kury, J. W. Adiabatic Expansion of High Explosive Detonation Products; UCRL-50422; Lawrence Livermore National Laboratory: Livermore, CA, 1968.

9. Johnson, G. R.; Cook, W. H. Fracture Characteristics of Three Metals Subjected to Various Strains, Strain Rates, Temperatures, and Pressures. *Journal of Engineering Fracture Mechanics* **1985**, *1*, 31–48.

10. Noh, W. F.; Woodward, P. SLIC (Simple Line Interface Calculation). *Lecture Notes in Physics*; vol. 59; Springer-Verlag, Berlin, 1976.

11. Bell, R. L.; Hertel Jr., E. S. *An Improved Material Interface Reconstruction Algorithm for Eulerian Codes*; SAND92-1716; Sandia National Laboratories: Albuquerque, NM, 1992.

12. Dobratz, B. M. *LLNL Explosives Handbook*; UCRL-5299; Lawrence Livermore Laboratory, University of California: Livermore, CA 1981.

INTENTIONALLY LEFT BLANK

Appendix A. Input Deck for RP-1 SC EBW Simulation

```
*
* id=1 - Starting baseline configuration
*
*eor*cgenin
*
ID=1: EBW Shaped Charge RP-1 SC
*
control
  ep
  mmp
endcontrol
*
mesh
  block  geometry 2dc  type e
    x0=0.0
      x1  n=650  dxf=0.001 rat=1.
    endx
    y0=-2.5
      y1  n=6600 dyf=0.001 rat=1.
    endy
*    xact=0.0,1.0
*    yact=0.0,5.0
  endblock
endmesh
*
insertion of material
  block 1
*
    package 'Cu Liner'
      material 1
      numsub 50
      insert circle
        center  0.0000  -0.4103
        radius  0.1524
      endinsert
      delete circle
        center  0.0000  -0.4103
        radius  0.1270
      enddelete
      delete uds
        p1      0.0000   0.0000
        p2      0.3835   0.0000
        p3      0.1320  -0.4865
        p4      0.1100  -0.4738
        p5      0.0000  -0.4738
      enddelete
    endpackage
*
    package 'Cu Liner'
      material 1
      numsub 50
```

```
      insert uds
        p1      0.3835   0.0000
        p2      0.3835  -0.0508
        p3      0.1320  -0.4865
        p4      0.1100  -0.4738
      endinsert
    endpackage
*
    package 'PETN Explosive'
      material 2
      numsub 50
      insert uds
        p1      0.3835  -0.0504
        p2      0.3835  -1.4111
        p3      0.0000  -1.4111
        p4      0.0000  -0.5627
        p5      0.1320  -0.4865
      endi
      delete circle
        center  0.0000  -0.4103
        radius  0.1524
      enddelete
    endpackage
*
    package 'Brass Case'
      material 3
      numsub 50
      insert box
        p1      0.3835   0.0000
        p2      0.5205  -1.4111
      endi
    endpackage
*
  endblock
endinsertion
*
epdata
*
  matep 1  johnson-cook copper     poisson 0.340
  matep 3  johnson-cook brass      poisson 0.340
  vpsave
  mix 3
endep
*
eos
  mat1 mgrun  copper
  mat2 jwl    petn1
  mat3 mgrun  brass
endeos
*
heburn
  material 2  d 5.17e5  pre 1.0e12
    dline 0.0000 -1.4111 to 0.3835 -1.4111  ti 0.0  radius 0.05
endheburn
*
tracer
  add  0.0   0.0
```

```
endtracer
*
*eor*cthin
*
ID=1: EBW Shaped Charge RP-1 SC
*
control
  tstop=50.e-6
  cpshift=900.
  rdumpf=3600
  ntbad 100000000
endcontrol
*
restart
  time=1.e-6
endr
*
cellthermo
  mmp2
endcell
*
convct
  convect=1
  interface=high
endc
*
discard
*  material 1  density  -.001 pressure 1.0e12  ton 1.1e-6
  material 2  density -0.01  pressure 5.0e6  ton  1.1e-6
  material 2  density 10.00  pressure 1.0e12  ton 2.8e-6 toff 2.9e-6
endd
*
edit
  shortt
    time=0.  dtf=10000.
  ends
  longt
    time=0.  dtf=10000.
  endl
  plott
    time=0.  dtf=0.05e-6
  endp
  plotdata
    volume
    mass
    temperature
    pressure
    velocity
  endplotdata
  restt
    time=0   dtf=1.e-6
  endr
  histc
    cycle=0  dcfreq=1
      htracer1
  endh
endedit
```

```
*
mindt
  time=0.  dtmin=1.0e-13
endm
*
fracts
  pressure
  pfrac1=-3.45e9
  pfrac2= -1e9
  pfrac3=-13.00e9
  pfmix =-5.0E20
  pfvoid=-5.0E20
endf
*
boundary
  bhydro
    block=1
      bxbot 0
      bxtop 2
      bybot 2
      bytop 2
    endb
  endh
endb
*
*eor*pltin
*
```

Appendix B. Input Deck for RP-4 SC EBW Simulation

```
*
* id=1 - Starting baseline configuration
*
*eor*cgenin
*
ID=1: EBW Shaped Charge RP-4 SC
*
control
  ep
  mmp
endcontrol
*
mesh
  block  geometry 2dc  type e
    x0=0.0
      x1  n=1500  dxf=0.001 rat=1.
    endx
    y0=-2.5
      y1  n=7500 dyf=0.001 rat=1.
    endy
*    xact=0.0,1.0
*    yact=0.0,5.0
  endblock
endmesh
*
insertion of material
  block 1
*
    package 'Cu Liner'
      material 1
      numsub 50
      insert circle
        center  0.0000  -1.3958
        radius  0.1270
      endinsert
      delete circle
        center  0.0000  -1.3958
        radius  0.0762
      enddelete
      delete uds
        p1      0.0000   0.0000
        p2      0.9525   0.0000
        p3      0.8425  -1.4593
        p4      0.8279  -1.4339
        p5      0.0000  -1.4339
      enddelete
    endpackage
*
    package 'Cu Liner'
      material 1
      numsub 50
```

```
      insert uds
        p1      0.8938   0.0000
        p2      0.9525   0.0000
        p3      0.1100  -1.4593
        p4      0.0660  -1.4339
      endinsert
    endpackage
*
    package 'PBX 9407 Explosive'
      material 2
      numsub 50
      insert uds
        p1      0.9525   0.0000
        p2      0.9525  -0.6653
        p3      0.4435  -1.9698
        p4      0.0000  -1.9698
        p5      0.0000  -1.5228
        p6      0.1100  -1.4593
      endi
      delete circle
        center  0.0000  -1.3958
        radius  0.1270
      enddelete
    endpackage
*
    package 'Aluminum Case'
      material 3
      numsub 50
      insert uds
        p1      0.9525   0.0000
        p2      1.2825   0.0000
        p3      1.2825  -0.8131
        p4      0.9033  -1.7850
        p5      0.9033  -1.9698
        p6      0.4435  -1.9698
        p7      0.9225  -0.6653
      endi
    endpackage
*
  endblock
endinsertion
*
epdata
*
  matep 1  johnson-cook copper     poisson 0.340
  matep 3  johnson-cook aluminum   poisson 0.330
  vpsave
  mix 3
endep
*
eos
  mat1 mgrun  copper
  mat2 jwl    pbx-9407
  mat3 sesame aluminum feos='/ha/cta/unsupported/CTH/CTH_9903/data/sesame'
endeos
*
heburn
```

```
  material 2  d 7.91e5  pre 1.0e12
    dline 0.0000 -1.9698 to 0.4435 -1.9698  ti 0.0  radius 0.05
endheburn
*
tracer
  add  0.0   0.0
endtracer
*
*eor*cthin
*
ID=1: EBW Shaped Charge RP-4 SC
*
control
  tstop=50.e-6
  cpshift=900.
  rdumpf=3600
  ntbad 100000000
endcontrol
*
*restart
*  time=2.e-6
*endr
*
cellthermo
  mmp2
endcell
*
convct
  convect=1
  interface=high
endc
*
discard
*  material 1  density  -.001 pressure 1.0e12  ton 1.1e-6
  material 2  density -0.01  pressure 5.0e6  ton  2.1e-6
  material 2  density 10.00  pressure 1.0e12  ton 4.0e-6 toff 4.1e-6
  material 3  density 10.00  pressure 1.0e12  ton 4.0e-6 toff 4.1e-6
endd
*
edit
  shortt
    time=0.  dtf=10000.
  ends
  longt
    time=0.  dtf=10000.
  endl
  plott
    time=0.  dtf=0.05e-6
  endp
  plotdata
    volume
    mass
    temperature
    pressure
    velocity
  endplotdata
  restt
```

```
    time=0   dtf=1.e-6
  endr
  histc
    cycle=0  dcfreq=1
      htracer1
  endh
endedit
*
mindt
  time=0.  dtmin=1.0e-13
endm
*
fracts
  pressure
  pfrac1=-3.45e9
  pfrac2= -1e9
  pfrac3=-4.00e9
  pfmix =-5.0E20
  pfvoid=-5.0E20
endf
*
boundary
  bhydro
    block=1
      bxbot 0
      bxtop 2
      bybot 2
      bytop 2
    endb
  endh
endb
*
*eor*pltin
*
```

Appendix C. Input Deck for RP-4 SFF EBW Simulation

```
*
* id=1 - Starting baseline configuration
*
*eor*cgenin
*
ID=1: EBW Shaped Forging Fragment RP-4 SFF
*
control
  ep
  mmp
endcontrol
*
mesh
  block  geometry 2dc  type e
    x0=0.0
      x1  n=1500  dxf=0.001 rat=1.
    endx
    y0=-2.5
      y1  n=7500 dyf=0.001 rat=1.
    endy
*    xact=0.0,1.0
*    yact=0.0,5.0
  endblock
endmesh
*
insertion of material
  block 1
*
    package 'Cu Liner'
      material 1
      numsub 50
      insert circle
        center  0.0000   2.6941
        radius  2.9108
      endinsert
      delete circle
        center  0.0000   2.6941
        radius  2.8575
      enddelete
      delete box
        p1       0.0000   0.0000
        p2      10.0000  10.0000
      enddelete
      delete box
        p1       0.9525 -10.0000
        p2      10.0000  10.0000
      enddelete
    endpackage
*
    package 'PBX 9407 Explosive'
      material 2
```

```
      numsub 50
      insert uds
        p1      0.0000   0.0000
        p2      0.9525   0.0000
        p3      0.9525  -0.6653
        p4      0.4435  -1.9698
        p5      0.0000  -1.9698
      endi
      delete circle
        center  0.0000   2.6941
        radius  2.9108
      enddelete
    endpackage
*
    package 'Aluminum Case'
      material 3
      numsub 50
      insert uds
        p1      0.9525   0.0000
        p2      1.2825   0.0000
        p3      1.2825  -0.8131
        p4      0.9033  -1.7850
        p5      0.9033  -1.9698
        p6      0.4435  -1.9698
        p7      0.9225  -0.6653
      endi
    endpackage
*
  endblock
endinsertion
*
epdata
*
  matep 1  johnson-cook copper     poisson 0.340
  matep 3  johnson-cook aluminum   poisson 0.330
  vpsave
  mix 3
endep
*
eos
  mat1 mgrun  copper
  mat2 jwl    pbx-9407
  mat3 sesame aluminum feos='/ha/cta/unsupported/CTH/CTH_9903/data/sesame'
endeos
*
heburn
  material 2  d 7.91e5  pre 1.0e12
    dline 0.0000 -1.9698 to 0.4435 -1.9698  ti 0.0  radius 0.05
endheburn
*
tracer
  add  0.0   0.0
endtracer
*
*eor*cthin
*
ID=1: EBW Shaped Forging Fragment RP-4 SFF
```

```
*
control
  tstop=50.e-6
  cpshift=900.
  nscycle=110000
  rdumpf=3600
  ntbad 1000000000
endcontrol
*
*restart
*  time=19.e-6
*endr
*
cellthermo
  mmp2
endcell
*
convct
  convect=1
  interface=high
endc
*
discard
*  material 1  density  -.001 pressure 1.0e12  ton 1.1e-6
  material 2  density -0.01  pressure 5.0e6  ton  2.1e-6
  material 2  density 10.00  pressure 1.0e12  ton 4.0e-6 toff 4.1e-6
  material 3  density 10.00  pressure 1.0e12  ton 4.0e-6 toff 4.1e-6
endd
*
vadd
  block=1
  tadd 20e-6
  yvel -2.9e5
endvadd
*
edit
  shortt
    time=0.  dtf=10000.
  ends
  longt
    time=0.  dtf=10000.
  endl
  plott
    time=0.  dtf=0.05e-6
  endp
  plotdata
    volume
    mass
    temperature
    pressure
    velocity
  endplotdata
  restt
    time=0   dtf=1.e-6
  endr
  histc
    cycle=0  dcfreq=1
```

```
      htracer1
  endh
endedit
*
mindt
  time=0.  dtmin=1.0e-13
endm
*
fracts
  pressure
  pfrac1=-3.45e9
  pfrac2= -1e9
  pfrac3=-4.00e9
  pfmix =-5.0E20
  pfvoid=-5.0E20
endf
*
boundary
  bhydro
    block=1
      bxbot 0
      bxtop 2
      bybot 2
      bytop 2
    endb
  endh
endb
*
*eor*pltin
```

Appendix D. Input Deck for RP-4 SC EBW 3-D Simulation

```
*
* id=1 - Starting baseline configuration
*
*eor*cgenin
*
ID=1: 3D EBW Shaped Charge RP-4 SC
*
control
  ep
  mmp
endcontrol
*
mesh
  block  geometry 3dr  type e
    x0=0.0
      x1  n=150 dxf=0.01 rat=1.
    endx
    y0=-2.5
      y1  n=750 dyf=0.01 rat=1.
    endy
    z0=0.0
      z1  n=150 dzf=0.01 rat=1.
    endz
*    xact=0.0,1.0
*    yact=0.0,5.0
  endblock
endmesh
*
insertion of material
  block 1
*
    package 'Cu Liner'
      material 1
      numsub 10
      insert sphere
        center  0.0000  -1.3958   0.0000
        radius  0.1270
      endinsert
      delete sphere
        center  0.0000  -1.3958   0.0000
        radius  0.0762
      enddelete
      delete r2dp
        ce1     0.0000   0.0000   0.0000
        ce2     0.0000   1.0000   0.0000
        p1      0.0000   0.0000
        p2      0.9525   0.0000
        p3      0.8425  -1.4593
        p4      0.8279  -1.4339
        p5      0.0000  -1.4339
      enddelete
```

```
    endpackage
*
    package 'Cu Liner'
      material 1
      numsub 10
      insert r2dp
        ce1     0.0000   0.0000   0.0000
        ce2     0.0000   1.0000   0.0000
        p1      0.8938   0.0000
        p2      0.9525   0.0000
        p3      0.1100  -1.4593
        p4      0.0660  -1.4339
      endinsert
    endpackage
*
    package 'PBX 9407 Explosive'
      material 2
      numsub 10
      insert r2dp
        ce1     0.0000   0.0000   0.0000
        ce2     0.0000   1.0000   0.0000
        p1      0.9525   0.0000
        p2      0.9525  -0.6653
        p3      0.4435  -1.9698
        p4      0.0000  -1.9698
        p5      0.0000  -1.5228
        p6      0.1100  -1.4593
      endi
      delete sphere
        center  0.0000  -1.3958   0.0000
        radius  0.1270
      enddelete
    endpackage
*
    package 'Aluminum Case'
      material 3
      numsub 10
      insert r2dp
        ce1     0.0000   0.0000   0.0000
        ce2     0.0000   1.0000   0.0000
        p1      0.9525   0.0000
        p2      1.2825   0.0000
        p3      1.2825  -0.8131
        p4      0.9033  -1.7850
        p5      0.9033  -1.9698
        p6      0.4435  -1.9698
        p7      0.9225  -0.6653
      endi
    endpackage
*
  endblock
endinsertion
*
epdata
*
  matep 1  johnson-cook copper     poisson 0.340
  matep 3  johnson-cook aluminum   poisson 0.330
```

```
  vpsave
  mix 3
endep
*
eos
  mat1 mgrun  copper
  mat2 jwl    pbx-9407
  mat3 sesame aluminum feos='/ha/cta/unsupported/CTH/CTH_9903/data/sesame'
endeos
*
heburn
  material 2  d 7.91e5  pre 1.0e12
    ddisk 0.0000 -1.9697 0.0000
       to 0.4435 -1.9697 0.0000
      and 0.0000 -1.9697 0.4435
      ti 0.0  radius 0.05
endheburn
*
tracer
  add  0.0   0.0   0.0
endtracer
*
*eor*cthin
*
ID=1: EBW Shaped Charge RP-4 SC
*
control
  tstop=25.e-6
  cpshift=900.
  rdumpf=3600
  ntbad 10000000000
endcontrol
*
restart
   time=4.0e-6
*  cycle=1911
endr
*
cellthermo
  mmp2
endcell
*
convct
  convect=1
  interface=smyra
endc
*
discard
  material 1  density  -.001 pressure 1.0e12  ton 4.3e-6
  material 2  density -0.01  pressure 5.0e6  ton  2.1e-6
  material 2  density 10.00  pressure 1.0e12  ton 4.3e-6 toff 4.4e-6
  material 3  density 10.00  pressure 1.0e12  ton 4.3e-6 toff 4.4e-6
endd
*
edit
  shortt
    time=0.  dtf=10000.
```

```
  ends
  longt
    time=0.  dtf=10000.
  endl
  plott
    time=0.  dtf=0.05e-6
  endp
  plotdata
    volume
    mass
    temperature
    pressure
    velocity
  endplotdata
  restt
    time=0   dtf=1.e-6
  endr
  histc
    cycle=0  dcfreq=1
      htracer1
  endh
endedit
*
mindt
  time=0.  dtmin=1.0e-13
endm
*
fracts
  pressure
  pfrac1=-3.45e9
  pfrac2= -1e9
  pfrac3=-4.00e9
  pfmix =-5.0E20
  pfvoid=-5.0E20
endf
*
boundary
  bhydro
    block=1
      bxbot 0
      bxtop 2
      bybot 2
      bytop 2
      bzbot 0
      bztop 2
    endb
  endh
endb
*
*eor*pltin
*
```

Acronyms

2-D	two-dimensional
3-D	three-dimensional
ANEOS	analytic equation of state package
ARL	U.S. Army Research Laboratory
EBW	exploding bridge wire
EFP	explosively formed penetrator
EOS	equation of state
JWL	Jones-Wilkins-Lee
RISI	Reynolds Industries Systems, Incorporated
SC	shaped charge
SCJ	shaped charge jet
SFF	self-forging fragment (old terminology for an EFP)

NO. OF COPIES	ORGANIZATION
*	ADMINISTRATOR DEFENSE TECHNICAL INFO CTR ATTN DTIC OCA 8725 JOHN J KINGMAN RD STE 0944 FT BELVOIR VA 22060-6218 *pdf file only
1	DIRECTOR US ARMY RSCH LABORATORY ATTN IMNE ALC IMS MAIL & REC MGMT 2800 POWDER MILL RD ADELPHI MD 20783-1197
1	DIRECTOR US ARMY RSCH LABORATORY ATTN AMSRD ARL CI OK TL TECH LIB 2800 POWDER MILL RD ADELPHI MD 20783-1197
1	INST FOR ADVNCD TCHNLGY THE UNIV OF TEXAS AT AUSTIN 4030-2 W BRAKER LN AUSTIN TX 78759-5329
3	INST FOR ADVNCD TECH ATTN S BLESS H FAN W REINECKE 4030-2 W BRAKER LN AUSTIN TX 78759
1	US MILITARY ACADEMY MATH SCI CTR EXCELLENCE MADN MATH LTC T RUGENSTEIN THAYER HALL WEST POINT NY 10996-1786
2	CDR US ARMY ARDEC ATTN AMSTA AR WEE C A DANIELS R FONG B3022 PICATINNY ARSENAL NJ 07806-5000
2	CDR US ARMY AVN & MISSILE CMD ATTN AMSAM RD PS WF S CORNELIUS S HOWARD REDSTONE ARSENAL AL 35898-5247
3	CDR US ARMY RSCH OFC ATTN S F DAVIS K IYER A RAJENDRAN PO BOX 12211 RSCH TRIANGLE PK NC 27709-2211

NO. OF COPIES	ORGANIZATION
1	COMMANDER NAVAL WEAPONS CTR ATTN N FASIG CODE 3261 CHINA LAKE CA 93555
1	CDR NAVAL SURF WARFARE CTR DAHLGREN DIVISION ATTN W E HOYE G02 17320 DAHLGREN RD DAHLGREN VA 22448-5100
2	CDR NAVAL SURF WARFARE CTR DAHLGREN DIVISION ATTN T SPIVAK G22 F ZERILLI 17320 DAHLGREN RD DAHLGREN VA 22448-5100
1	AIR FORCE ARMAMENT LAB ATTN AFATL DLJR D LAMBERT EGLIN AFB FL 32542-6810
2	DARPA ATTN W SNOWDEN S WAX 3701 N FAIRFAX DR ARLINGTON VA 22203-1714
2	LOS ALAMOS NATL LAB ATTN P HOWE MS P915 PO BOX 1663 LOS ALAMOS NM 87545
2	LOS ALAMOS NATL LAB ATTN L HULL MS A133 J V REPA MS A133 PO BOX 1663 LOS ALAMOS NM 87545
5	SANDIA NATL LAB ATTN R BELL MS0836 9116 D CRAWFORD MS0836 9116 E HERTEL MS0836 9116 S SILLING MS0820 9232 D PRECE MS 0819 ALBUQUERQUE NM 87185-0100
3	DIR LAWRENCE LIVERMORE NATL LAB ATTN D BAUM L099 M MURPHY C SIMONSON MS PO BOX 808 MS L35 LIVERMORE CA 94550

NO. OF COPIES	ORGANIZATION
1	DIR LAWRENCE LIVERMORE NATL LAB ATTN R VAROSH L149 PO BOX 808 LIVERMORE CA 90550
2	SOUTHWEST RSCH INST ATTN C ANDERSON J WALKER PO DRAWER 28510 SAN ANTONIO TX 78228-0510
2	AEROJET ATTN J CARLEONE S KEY PO BOX 13222 SACRAMENTO CA 95813-6000
1	CMPTNL MECHS CNSLTNTS ATTN J A ZUKAS PO BOX 11314 BALTIMORE MD 21239-0314
3	DETK ATTN R CICCARELLI W FLIS M MAJERUS 3620 HORIZON DR KING OF PRUSSIA PA 19406
1	RAYTHEON MSL SYS CO ATTN T STURGEON BLDG 805 MS D4 PO BOX 11337 TUCSON AZ 85734-1337
1	TEXTRON DEFENSE SYSTEMS ATTN C MILLER 201 LOWELL ST WILMINGTON MA 01887-4113
1	D R KENNEDY & ASSOC INC ATTN D KENNEDY PO BOX 4003 MOUNTAIN VIEW CA 94040
1	LOCKHEED MARTIN ELECTRONICS & MISSILES ATTN G W BROOKS 5600 SAND LAKE RD MP 544 ORLANDO FL 32819-8907
4	GD OTS ATTN C ENGLISH T GRAHAM D A MATUSKA J OSBORN 4565 COMMERCIAL DR A NICEVILLE FL 32578

NO. OF COPIES	ORGANIZATION
2	GD OTS ATTN D BOEKA N OUYE 400 ESTUDILLO AVE STE 100 SAN LEANDRO CA 94577-0205
1	ZERNOW TECHNICAL SVS INC ATTN L ZERNOW 425 W BONITA AVE STE 208 SAN DIMAS CA 91773
1	PM JAVELIN PO ATTN SSAE FS AM EG C ALLEN REDSTONE ARSENAL AL 35898-5720
1	PM TOW ATTN SFAE TS TO J BIER REDSTONE ARSENAL AL 35898-5720
1	HALLIBURTON ENERGY SVCS JET RESEARCH CENTER ATTN D LEIDEL PO BOX 327 ALVARADO TX 76009-9775
1	NORTHROP GRUMMAN ATTN DR D PILLASCH B57 D3700 PO BOX 296 1100 W HOLLYVALE ST AZUSA CA 91702
1	INTRNTL RSRCH ASSOC ATTN D ORPHAL 4450 BLACK AVE PLEASANTON CA 94566-6105
1	JIM VAROSH TELEDYNE RISI INC PO BOX 359 TRACY CA 95378
	ABERDEEN PROVING GROUND
1	DIRECTOR US ARMY RSCH LABORATORY ATTN AMSRD ARL CI OK (TECH LIB) BLDG 4600
1	US ARMY RESEARCH LABORATORY ATTN AMSRD ARL WM J SMITH BLDG 4600
1	US ARMY RESEARCH LABORATORY ATTN AMSRD ARL WM EG E SCHMIDT BLDG 4600

NO. OF COPIES	ORGANIZATION
2	US ARMY RESEARCH LABORATORY ATTN AMSRD ARL WM MB W DEROSSET R DOWDING BLDG 4600
1	US ARMY RESEARCH LABORATORY ATTN AMSRD ARL WM T B BURNS BLDG 309
1	US ARMY RESEARCH LABORATORY ATTN AMSRD ARL WM TA W GILLICH BLDG 309
11	US ARMY RESEARCH LABORATORY ATTN AMSRD ARL WM TA W GOOCH M BURKINS (5 CYS) T HAVEL M KEELE D KLEPONIS J RUNYEON S SCHOENFELD BLDG 393
4	US ARMY RESEARCH LABORATORY ATTN AMSRD ARL WM TB P BAKER R BANTON R LOTTERO J STARKENBERG BLDG 309
24	US ARMY RESEARCH LABORATORY ATTN AMSRD ARL WM TC G BOYCE R COATES T FARRAND E KENNEDY K KIMSEY L MAGNESS S SCHRAML D SCHEFFLER (6 CYS) B SORENSEN R SUMMERS C WILLIAMS W WALTERS (6 CYS) R ANDERSON M FERMEN-COKER BLDG 309
6	US ARMY RESEARCH LABORATORY ATTN AMSRD ARL WM TD Y HUANG T WEERASOORIYA T W BJERKE E RAPACKI S SEGLETES M RAFTENBERG BLDG 4600
1	US ARMY RESEARCH LABORATORY ATTN AMSRD ARL SL BE A PRAKASH BLDG 390A